Supplementary Information

to

"Nanoscale Viscosity of Cytoplasm Is Conserved In Human Cell Lines"

Karina Kwapiszewska,[*a] *Krzysztof Szczepański,*[a] *Tomasz Kalwarczyk,*[a] *Bernadeta Michalska,*[b] *Paulina Patalas-Krawczyk,*[b] *Jędrzej Szymański,*[b] *Tomasz Andryszewski,*[a] *Michalina Iwan,*[a] *Jerzy Duszyński*[b] *and Robert Hołyst* [*a]

[a] Institute of Physical Chemistry, Polish Academy of Sciences, Kasprzaka 44/52, Warsaw, POLAND

[b] Nencki Institute of Experimental Biology, Pasteura 3, Warsaw, POLAND

Corresponding Authors

* kkwapiszewska@ichf.edu.pl, rholyst@ichf.edu.pl

SI 1. Materials and Methods

Fluorescent tracers. PEG-coated fluorescent silica nanoparticles filled with Rhodamine B were custom-synthetized for this research by Siliquan (https://siliquan.com/). The nanoparticles were designed as fluorescent cores of radii ~20 nm, doped in non-fluorescent silica shells, to avoid the impact of relatively big fluorescent objects on apparent diffusion times.[1,2] TRITC-labelled dextrans of 4,4 kDa, 20 kDa, 40 kDa, 65-75 kDa, and 155 kDa were purchased from Sigma-Aldrich. Calcein-AM was purchased from Sigma-Aldrich. EGFP protein was expressed in cells from the pcDNA3-EGFP plasmid (Addgene).

Cell culture. Following ATCC human cell lines were used in the research: cervical adenocarcinoma (HeLa), lung carcinoma (A549), adenocarcinoma from the mammary gland (MCF-7), hepatocellular carcinoma (HepG2), bone osteosarcoma (U2-OS) and normal small airway epithelial cells (HSAEC). Human skin primary fibroblasts were obtained from the Coriell repository.

The majority of cells were cultured in DMEM (Institute of Immunology and Experimental Technology, Wrocław, Poland) supplemented with $10\%_{vol}$ fetal bovine serum, L-glutamine (2 mM), penicillin (100 mg/ml) and streptomycin (100 mg/ml) (Sigma-Aldrich). Medium for MCF-7 cells was additionally supplemented with 0.01 mg/mL insulin (Sigma-Aldrich). HSAEC were cultured using media recommended for this cell line and purchased from ATCC. Cells were maintained at 37°C in a 5% CO_2 humidified atmosphere. The passage was performed at ~80% confluence (every 2-4 days, depending on cell line) using 0.25% Trypsin-EDTA solution (Sigma-Aldrich) and PBS (Sigma-Aldrich).

Probe introduction. Probes were introduced into cell cytosol via spontaneous uptake (Calcein-AM), microinjection (dextrans, nanoparticles), or transfection (EGFP). For transfection cells were grown on 8-chamber cover glass Lab-Tek® slide to ~30% of confluence. Transfection was performed using JetPRIME® reagent (Polyplus Transfection) according to the manufacturer's protocol. FCS experiments were performed 24 hours after transfection. For microinjection, cells were grown on 35 mm glass-bottom dishes to approx. 30% of confluence. Microinjection was performed by Femtojet® system (Eppendorf), with glass capillaries of diameters <1 µm, prepared using micropipette puller (P-1000, Sutter Instrument). The concentrations of injected solutions were in the range of 5-40 µM (in PBS). Approx. 1000 cells were injected per experiment with settings: injection pressure 160 hPa, injection time 0.2 s, and compensation pressure 30 hPa. FCS measurements were performed 1 h after microinjection. Calcein-AM was introduced directly to medium to a final concentration of 1nM. Uptake occurred within 20 minutes.

Fluorescence correlation spectroscopy (FCS) and raster image correlation spectroscopy (RICS). FCS and RICS were performed using setup based on a confocal microscope (Nikon Eclipse TE2000U, Nikon, Japan) coupled with Pico Harp 300 FCS equipment (PicoQuant, Germany). Measurements were performed in a climate chamber (Okolab, Italy), providing temperature control (36 ± 0.5 °C) and the atmosphere of required composition and humidity. He-Ne laser (543 nm) and pulsed diode laser (481 nm) were used as light sources. Power was kept in the ranges of 5-20 µW for 543 nm laser and 1-5 µW for 481 nm laser. Probes were observed and measured through a 60 x (N.A. 1.2) objective with water immersion. The fluorescent signal was collected by Single Photon Avalanche Diodes (MPD and PerkinElmer). Each experiment was preceded by a calibration using Rhodamine B (λ_{ex} = 543 nm, Sigma-Aldrich) or Rhodamine 110 (λ_{ex} = 481 nm, Sigma-Aldrich) dissolved in a solution of $2.5\%_{wt}$ glucose in PBS.[3] The objective correction collar was adjusted to provide optimal FCS read-out, and RhoB diffusion was used for precise characterization of focal volume size and shape. For experiments on cells, the cell culture medium was replaced with PBS containing calcium and magnesium ions (Sigma-Aldrich) to avoid background signal. For

FCS, the detection volume was positioned in a cytoplasmic area of a cell using the imaging mode of the microscope. All cells picked for measurements adhered to the glass surface, and the focal volume was positioned approx.. 2 µm above the glass. Data was acquired using SymphoTime software. Single measurements took 15 seconds to 10 minutes, depending on the diffusion coefficient of the probe. For RICS square region of interest (ROI) was defined in the cytoplasmic area of the cell. Images were taken using the FLIM module of SymphoTime. A series of images were acquired with the following parameters: ROI size – 20x20 µm, image size – 256x256 px, pixel dwell – 12 µs. Series of 50 subsequent images was taken at each ROI.

Data fitting and calculations. FCS autocorrelation curves were calculated from raw data using SymphoTime software. Next, autocorrelation curves were fitted with a proper model (3D normal diffusion or 3D anomalous diffusion, depending on a probe)[3] using QuickFit 3.0 software. For RICS data analysis, we used the SimFCS software provided by prof. Gratton, whose team was the first to introduce the RICS method.[4] Length-scale dependent viscosity model, was fitted to experimental data using Gnuplot 5.0 software.

Cell staining and confocal imaging. Staining was performed on formaldehyde-fixed, and Triton-X permeabilized cells. Actin was stained using phalloidin-Alexa647 conjugate (Thermo Fisher Scientific). Tubulin was stained using paclitaxel-Oregon Green conjugate (Thermo Fisher Scientific). The endoplasmic reticulum was visualized using antibody-based SelectFX™ Alexa Fluor™ 488 Endoplasmic Reticulum Labeling Kit (Thermo Fisher Scientific). Nucleus was stained using DAPI (ThermoFisher Scientific). After staining (according to manufacturer protocol), cells were mounted in PBS for imaging. Confocal imaging was performed by Nikon A1 confocal microscope based on Eclipse Ti inverted microscope. Images were analyzed using NIS-Elements AR 4.13.04 software. The image for each fluorophore was acquired separately. Image post-processing and quantitative analysis were performed in ImageJ software.

SI 2. Characteristics of fluorescent tracers

All tracers used in experiments are listed in Table SI.2. Depending on a probe, a different way of introduction to cells were applied: (1) passive inflow of Calcein-AM, (2) transfection of a plasmid encoding fluorescent protein, or (3) microinjection of dextrans and PEG-ylated nanoparticles. This set of tracers covered length-scales of from 1 to >160 nm.

Table SI.2 Fluorescent tracers used for probing nanoviscosity.

Tracer	Label	r_p [nm]	Method of r_p determination	Method of introduction to the cytoplasm
Calcein	Calcein	0.65	Literature[5]	Passive inflow
Dextran 4.4 kDa	TRITC	1.3	FCS measurement	Microinjection
Dextran 20 kDa	TRITC	3.8	FCS measurement	Microinjection
Dextran 40 kDa	TRITC	4.9	FCS measurement	Microinjection
Dextran 65-85 kDa	TRITC	5.6	FCS measurement	Microinjection
Dextran 155 kDa	TRITC	8.6	FCS measurement	Microinjection
EGFP	EGFP	2.3	HydroPro modelling	Transfection and biosynthesis
EGFP-apoferritin	EGFP	9.4	HydroPro modeling	Transfection and biosynthesis
Nanoparticles 1	TRITC	21	FCS measurement	Microinjection
Nanoparticles 2	TRITC	34	FCS measurement	Microinjection
Nanoparticles 3	TRITC	68	FCS measurement	Microinjection
Nanoparticles 4	TRITC	81	FCS measurement	Microinjection

SI 3. Autocorrelation curve fitting

The general form of the autocorrelation function (ACF) describing translational diffusion of the tracer is as follows:

$$G(\tau) = \frac{1}{N}\sum_{i}^{n} A_i \frac{1}{1+\left(\frac{\tau}{\tau_{D,i}}\right)^{\alpha_i}} \frac{1}{\sqrt{1+\frac{1}{\kappa^2}\left(\frac{\tau}{\tau_{D,i}}\right)^{\alpha_i}}}$$

Here N stands for the average number of fluorescent probes inside the focal volume, τ_D is the time of diffusion of an average probe across the focal volume, A_i corresponds to the amplitude of the i^{th} component, κ is the aspect ratio of the focal volume, and α is the anomality parameter reflecting polydispersity of the probe.[3] The ACF used for fitting FCS data obtained in cells differed according to the probe type. The proper ACF was considered for each example of tracer separately, concerning possible interactions with intracellular content.[6] Variants of ACF, together with justifications for each of the probe's groups, were listed in Table SI.3. Example fits of the tracers of three different groups are presented in Fig. SI. 3.

Table SI. 3

Tracer group	α	i	Diffusion type	Justification of the model of choice
Dyes	1	2	Two component free diffusion	Calcein is a small organic molecule, which can interact with cellular content. These unspecific interactions result in a two-component type of diffusion, where the first component reflects free dye, and the second is for the dye bound to intracellular content.
Proteins	1	1	One component free diffusion	Fluorescent proteins are monodisperse probes, with practically no interactions with cellular content. Thus, free, undisturbed diffusion is observed.
Dextrans Nanoparticles	<1	1	One component anomalous diffusion	Due to the technical issues, dextrans and nanoparticles always exhibit some degree of polydispersity. While polydispersity of the majority of probes does not have its contribution to ACF in water, it becomes more pronounced in the cytoplasm.[3] The anomality parameter α decreases with an increasing polydispersity of the probe.

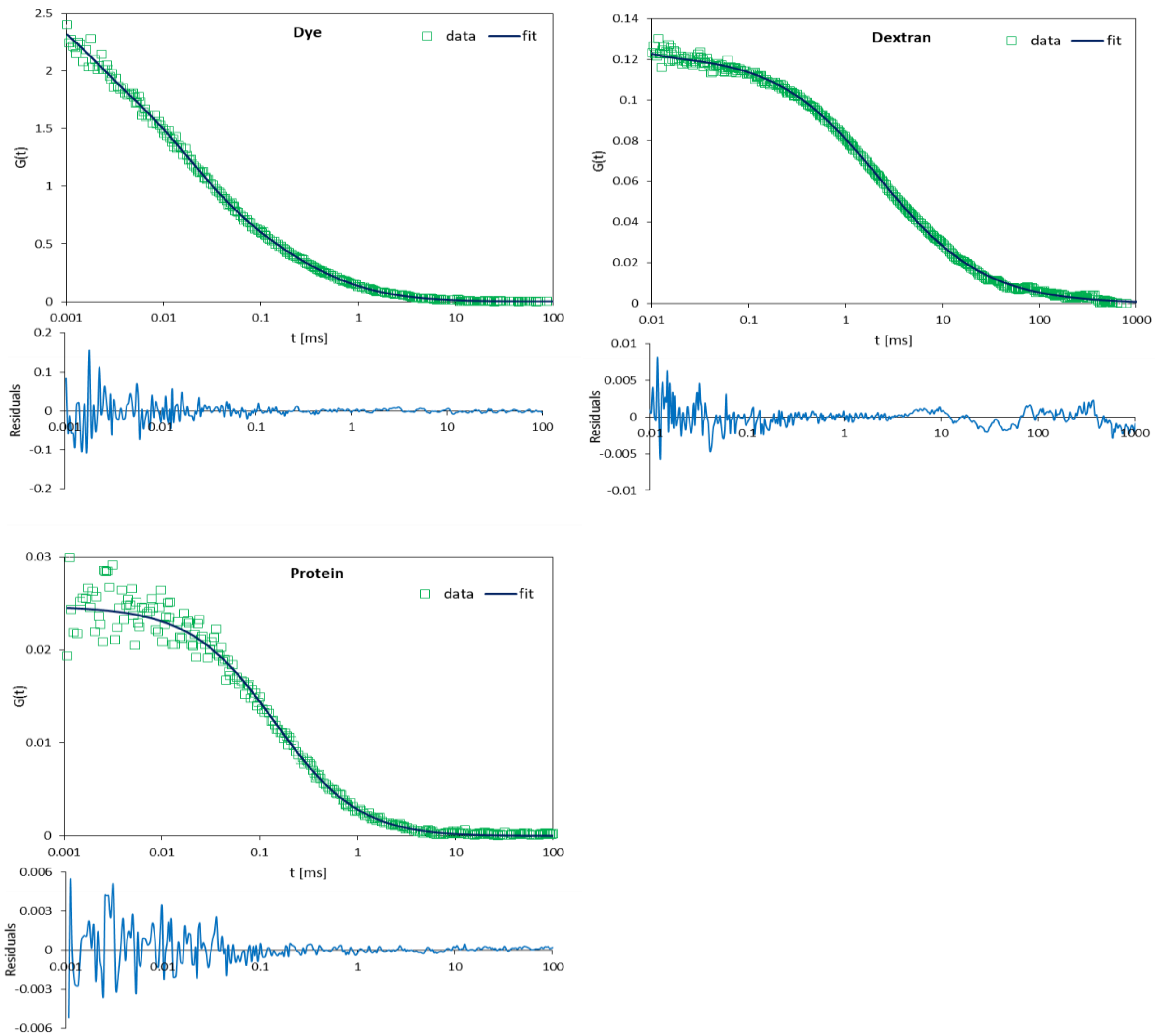

Figure SI 3. Examples of autocorrelation curves and fitted autocorrelation functions for representatives of three groups of tracers: (Dye) Calcein-AM in the cytoplasm of HSAEC cells, fitted with two component free diffusion model; (Protein) EGFP in cytoplasm of HeLa cells, one component free diffusion model; (Dextran) dextran 155 kDa in the cytoplasm of HeLa cells, one component anomalous diffusion model.

In all model variants, τ_D is the fitting parameter of interest. Diffusion coefficients of the probes are derived from the equation:

$$D = \frac{{\omega_{xy}}^2}{4\tau_D}$$

Where D is the diffusion coefficient of a probe, and ω_{xy} is a dimension of a focal volume determined during the calibration step (see SI.1).

SI 4. Variability of nanoviscosity: intracellular vs. intercellular.

To check whether the localization inside the cell cytoplasm impacts the obtained data, we performed additional measurements. Two probes were used for this control experiment: dextran 40 kDa and dextran 155 kDa, probing length-scales of 10 nm and 16 nm, respectively. Inside a single HeLa cell, 3-6 measurements were taken (see Fig. SI 4). The number of measurements per cell depended on the size of the cell and availability of cytoplasmic region to FCS measurements (excluding nucleus and areas of a high density of vesicles). We aimed to measure distinctively in different areas.

The obtained relative standard deviation of the relative diffusion coefficient varied from 6.24 % to 15.29 %. For dextran 40 kDa, the intracellular standard deviation was, on average, 12.6%, while intracellular standard deviation (all experiment on dextran 40 kDa in HeLa) was 12.7%. For dextran 155 kDa, the intracellular standard deviation was, on average, 11.4%, while the intracellular standard deviation was 10.1%.

We assume that our experimental protocol (FCS, its calibration, and data fitting) gives an uncertainty of 10%. Thus, obtained values of standard deviations are all close to experimental error. Basing o this, we can conclude that our experimental procedure, of probing different cells in the population, is reliable.

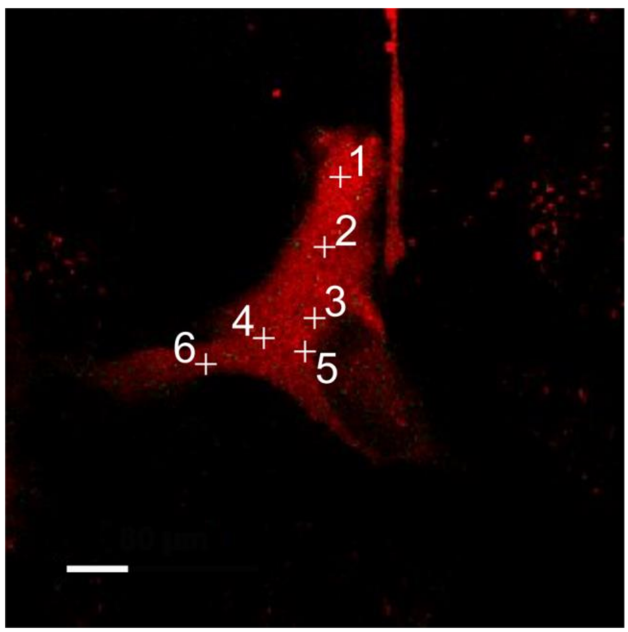

Fig SI 4. HeLa cell filled with dextran 40 kDa used for the experiments. Measurement spots are marked with "+". Scale bar corresponds to 10 µm.

SI 5. Comparison of cytoplasmic viscosity reported in different studies.

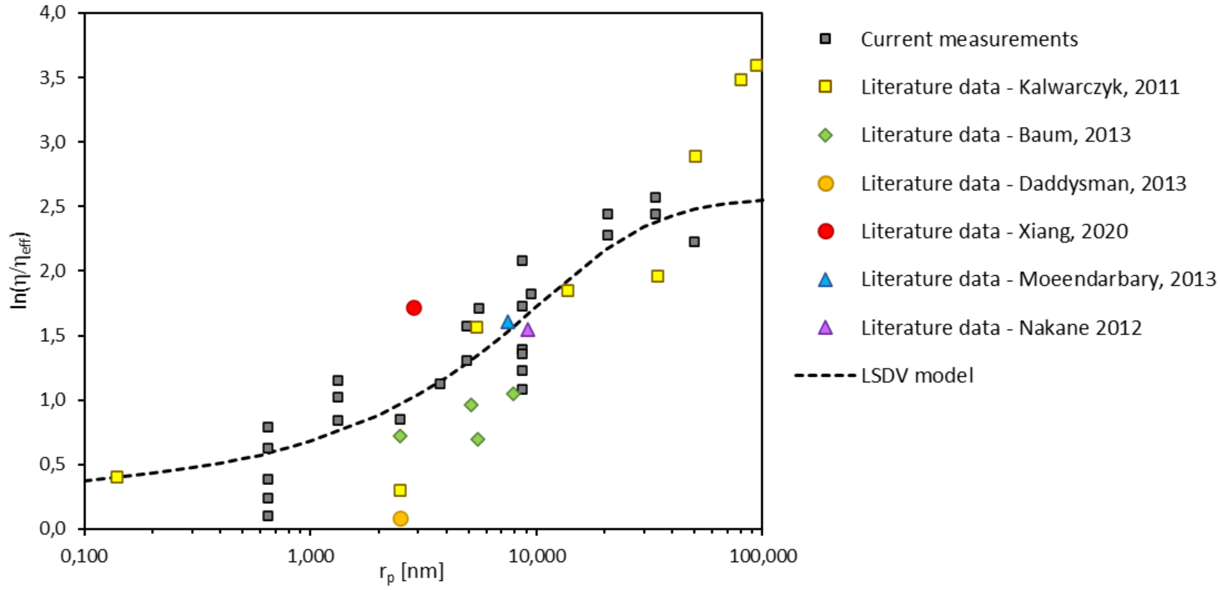

Fig. SI 5. The measurements and a model resulting from our study, compared to the literature data.[7–12] Scattered data measured with different methods are in good agreement with the LSDV curve developed in the current study. Literature data picked for comparison: Kalwarczyk, 2011 – literature data analyzed and discussed in our previous paper, all data points for HeLa cells, mostly FRAP;[8] Baum, 2013 – proteins in U2Os cells, modified FCS;[7] Daddysman, 2013 – GFP in HeLa, FRAP (anomalous diffusion);[9] Xiang, 2020 – the protein in PtK2 cells, custom single-molecule displacement mapping;[10] Moeendarbary, 2013 – EGFP decamer in HeLa, FRAP;[11] Nakane, 2012 – bovine serum albumin covered quantum dots in HeL, FCS.[12]

SI 6. Types of cells used in experiments

Table SI.6. Cell lines used in the present study grouped in categories possibly affecting their nanoviscosity

Tissue		Disease	
epithelial	mesenchymal	normal	cancer
Hep-G2 MCF-7 A549 HSAEC	Fibroblasts U2-Os	HSAEC Fibroblasts	HeLa HepG2 MCF-7 A549 U2-Os
Gender of a donor		**Age of a donor**	
female	male	young (< 20 years)	adult
HeLa MCF-7 U2-Os	Hep-G2 A549 HSAEC	Hep-G2 U2-Os	HeLa MCF-7 A549 HSAEC

SI 7. Effect of passage number on the viscosity of fibroblasts

We considered cell culture aging as one of the factors possibly affecting cytoplasmic viscosity of primary skin fibroblasts. Primary cells are known to degenerate after some time in culture. The lifespan of a culture is measured in passages, and it is recommended to perform experiments at the lowest possible passage number. As the nanoviscosity measured in the cytosol of fibroblasts differed from other cell lines, we considered the age of culture as a possible causing factor. We plotted values of relative viscosity measured in fibroblasts in different passages (passage 3-7, Fig. SI.4). No trend was visible – there was no dependence between the passage number and increase or decrease of cytoplasmic nanoviscosity.

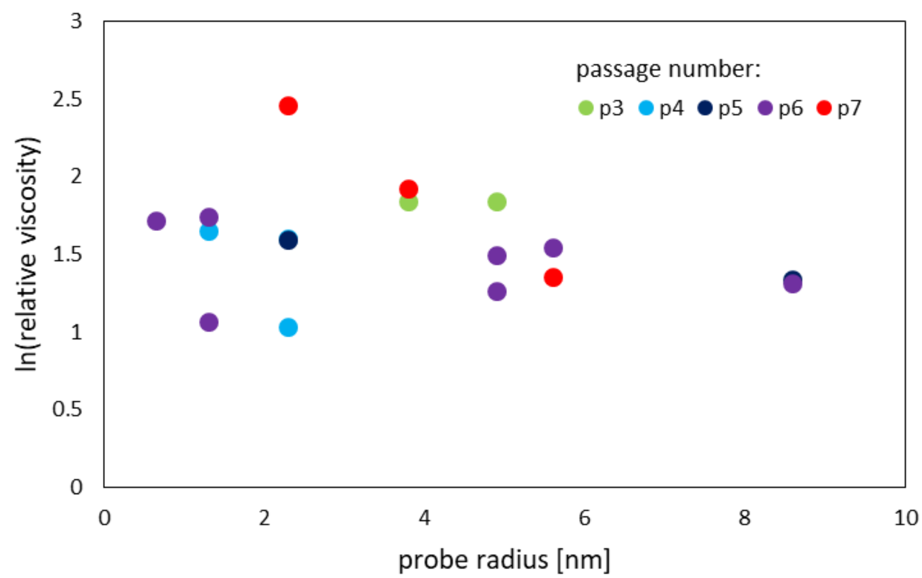

Fig SI 7. Nanoviscosity measured in fibroblasts at different passage numbers – no trend is visible.

SI 8. Quantification of ER abundance

Confocal images of immunostained ER were used for quantification of ER abundance. The analysis was performed using ImageJ software. First, the images were cropped into smaller pieces, containing only the ER area. Next, the small images were binarized using thresholding, reflecting original ER architecture. The number of white and black pixels was counted, and the percentage of white pixels corresponded to ER abundance. The procedure was schematically presented in Fig. SI 5.

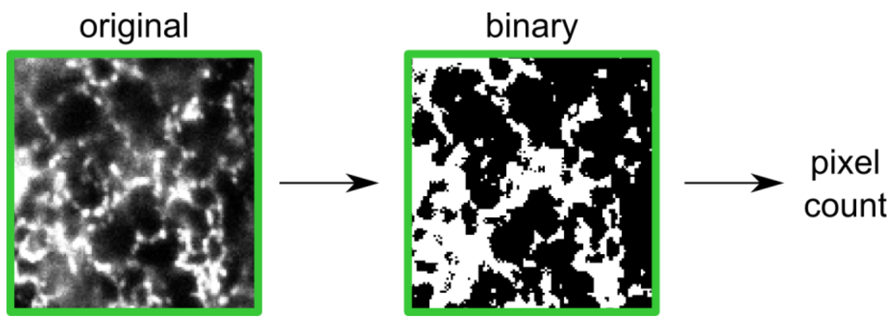

Fig. SI 8. A scheme of ER abundance quantification

References

(1) Deptuła, T.; Buitenhuis, J.; Jarzębski, M.; Patkowski, A.; Gapinski, J. Size of Submicrometer Particles Measured by FCS : Correction of the Confocal Volume. *Langmuir* **2015**, 31, 6681–6687.

(2) Gapinski, J.; Jarzębski, M.; Buitenhuis, J.; Deptula, T.; Mazuryk, J.; Patkowski, A. Structure and Dimensions of Core−Shell Nanoparticles Comparable to the Confocal Volume Studied by Means of Fluorescence Correlation Spectroscopy. *Langmuir* **2016**, 32, 2482–2491.

(3) Kalwarczyk, T.; Kwapiszewska, K.; Szczepanski, K.; Sozanski, K.; Szymanski, J.; Michalska, B.; Patalas-Krawczyk, P.; Duszynski, J.; Holyst, R. Apparent Anomalous Diffusion in the Cytoplasm of Human Cells: The Effect of Probes' Polydispersity. *J. Phys. Chem. B* **2017**, 121 (42), 9831–9837.

(4) Rossow, M. J.; Sasaki, J. M.; Digman, M. A.; Gratton, E. Raster Image Correlation Spectroscopy in Live Cells. *Nat Protoc.* **2009**, 377 (2), 364–377.

(5) Kwapiszewska, K.; Kalwarczyk, T.; Michalska, B.; Szczepański, K.; Szymański, J.; Patalas-Krawczyk, P.; Andryszewski, T.; Iwan, M.; Duszyński, J.; Hołyst, R. Determination of Oligomerization State of Drp1 Protein in Living Cells at Nanomolar Concentrations. *Sci. Rep.* **2019**, 9 (1), 5906.

(6) Zhang, X.; Sisamakis, E.; Sozanski, K.; Holyst, R. Nanoscopic Approach to Quantification of Equilibrium and Rate Constants of Complex Formation at Single-Molecule Level. *J. Phys. Chem. Lett.* **2017**, 8 (23), 5785–5791.

(7) Baum, M.; Erdel, F.; Wachsmuth, M.; Rippe, K. Retrieving the Intracellular Topology from Multi-Scale Protein Mobility Mapping in Living Cells. *Nat. Commun.* **2014**, 5, 1–12.

(8) Kalwarczyk, T.; Ziębacz, N.; Bielejewska, A.; Zaboklicka, E.; Koynov, K.; Szymański, J.; Wilk, A.; Patkowski, A.; Gapiński, J.; Butt, H.-J.; Hołyst, R. Comparitive Analysis of Viscosity of Complex Liquids and Cytoplasm of Mammalian Cell at the Nanoscale. *Nano Lett.* **2011**, 11, 2157–2163.

(9) Daddysman, M. K.; Fecko, C. J. Revisiting Point FRAP to Quantitatively Characterize Anomalous Diffusion in Live Cells. *J. Phys. Chem. B* **2013**, 117 (5), 1241–1251.

(10) Xiang, L.; Chen, K.; Yan, R.; Li, W.; Xu, K. Single-Molecule Displacement Mapping Unveils Nanoscale Heterogeneities in Intracellular Diffusivity. *Nat. Methods* **2020**, 17, 524–530.

(11) Moeendarbary, E.; Valon, L.; Fritzsche, M.; Harris, A. R.; Moulding, D. A.; Thrasher, A. J.; Stride, E.; Mahadevan, L.; Charras, G. T. The Cytoplasm of Living Cells Behaves as a Poroelastic Material. *Nat. Mater.* **2013**, 12 (3), 253–261.

(12) Nakane, Y.; Sasaki, A.; Kinjo, M.; Jin, T. Bovine Serum Albumin-Coated Quantum Dots as a Cytoplasmic Viscosity Probe in a Single Living Cell. *Anal. Methods* **2012**, 4 (7), 1903–1905.